Investigating the Mechanistic Effects of Medication on Pulmonary Hypertension

Malak Sabry[1,2], Pablo Lamata[1], Ahmed Hassan[2,3], Onaiho Ojo[4], Magdi H Yacoub[2,5], Adelaide de Vecchi[1]

[1] Dept. of Biomedical Engineering, King's College London, London, UK
[2] Aswan Heart Research Centre, Aswan, Egypt
[3] Cardiology Dept., Cairo University, Cairo, Egypt
[4] GKT School of Medical Education, King's College London, London, UK
[5] National Heart and Lung Institute, Imperial College London, London, UK

Abstract

Pulmonary Hypertension (PH) affects the right heart, and is characterized by high mean pulmonary arterial pressure (mPAP). Treprostinil is a drug for PH that dilates downstream blood vessels, reducing pressure, peripheral vascular resistance (PVR), and right ventricle (RV) workload. Combining clinical data and model-derived metrics, this work aims to better understand the impact of Treprostinil in the interplay between RV, proximal, and peripheral arteries. Data from two PH patients undergoing treatment, a responder and a non-responder, were compared. Metrics of RV function, proximal pulmonary artery (PA), RV-PA coupling, and PVR, were analyzed. Compared to the responder, the non-responder had worsened RV function (15% increase vs 20% decrease in end-systolic volume), impaired coupling (0.36 vs 0.60), and increased mPAP (89 vs 46mmHg) despite decreased PVR (38 vs 13 WU), significant dilation of proximal PA (15-45% vs 1-6%) with minimal angulation changes, and increased arterial stiffness (pulse wave velocity: 8 vs 4.2 m/s). Findings suggest that Treprostinil is more effective in earlier stages of PH and that the large PA dilation in the non-responder might be a compensatory mechanism for insufficient downstream vasodilation. The study highlights the potential of computational models to provide markers to assess treatment responses and disease progression in PH, however further research with larger patient groups is needed.

1. Introduction

Pulmonary Hypertension (PH) is a chronic condition characterized by an abnormally elevated mean pulmonary arterial pressure (mPAP) exceeding 20 mmHg at rest. This persistent elevation triggers progressive remodelling of the pulmonary vasculature, and an eventual right ventricular (RV) dysfunction[1]. PH is also associated with an impaired coupling between the right ventricle contractility and pulmonary afterload. Defining contractility as the end-systolic elastance (E_{es}), and afterload as the arterial elastance (E_a), the ratio E_{es}/E_a encapsulates the RV-PA coupling efficiency, with healthy values close to 1 [1]. To maintain coupling, both the RV and the PA must adapt as PH progresses. This concept of coupling emerges from the inherent anatomical and physiological interplay between ventricle and vasculature, requiring us to look at them as a cohesive functional unit, rather than separate entities. Treprostinil is a medication approved for treating Group I PH. Its primary mode of action involves directly dilating downstream blood vessels. This vasodilation leads to a decrease in pulmonary artery resistance and RV afterload, ultimately enhancing cardiac output [2]. The reduction in afterload after 3 months on Treprostinil has also been shown to normalize the RV-PA coupling to baseline values [3]. Nevertheless, the response to Treprostinil can be negative, there is a need to predict irreversible RV failure. RV-PA coupling has been proposed as an index to predict response, but with negative findings [4]. In this context, the study of how the medication acts on arterial flow dynamics and their interplay with ventricular mechanics is a sound approach to understand if reverse modelling is possible. Virtual, *in-silico*, replicas of cardiovascular features offer a framework to systematically analyze the intricate interplay between the different components of the ventriculo-arterial coupling system [5]. By comparing data-driven models of a responder and a non-responder case, the paper aims to explore the impact of Treprostinil on four cardiovascular components: RV, proximal PA, RV-PA coupling, and peripheral vascular resistance (PVR).

2. Methods

2.1. Data

Data from two confirmed Group I PH patients undergoing treatment using Treprostinil, a non-responder (Case 1) and a responder (Case 2), was used. Computed tomography (CT) and magnetic resonance imaging (MRI) were performed on the RV and PA. Pressure tracings were obtained using a Judkins right coronary catheter. Data from their first visit, before the drug was administered, and from their follow-up exam (F-U) after two years on Treprostinil were analyzed and used to calibrate computational fluid dynamics (CFD) models. All subjects participated under informed consent and data access was granted through the Aswan Heart Centre Research Ethics Committee (REC code: 20210804MYFAHC - VAPH - 20211025).

Table 1. Cohort (mPAP in mmHg, PVR in WU).

Case	Sex	Age	Visit	mPAP	PVR
1	F	23	Initial	83	41
		25	F-U	89	38
2	F	32	Initial	55	16
		34	F-U	46	13

2.2. Pressure-Volume Loops

RV pressure tracings were extracted from catheter data, and synchronized using the ECG with the volume curve obtained from short-axis MR images of the RV over a cardiac cycle. Pressure-Volume (PV) loops were then obtained, and the single-beat method was implemented to calculate ventricular elastance, arterial elastance, and RV-PA coupling using only one PV loop [6].

2.3. Right Ventricular Function

RV functional parameters such as end-systolic and end-diastolic volumes (ESV and EDV), stroke volume (SV), and ejection fraction (EF) were computed from the volume curves. RV energetics were computed according to [7]. Stroke work (SW), referring to the work done by the ventricle to eject blood during systole, was estimated as the area of the PV loop. Stroke power (SP) was then calculated by dividing the SW by the contraction time of the ventricle. The RV stroke power output (RVSPO ratio), representing the amount of ventricular power actually transferred to the MPA during systolic ejection, i.e. the efficiency of the energetic transfer, was calculated as the ratio between the actual power output on the MPA side (PO) and the SP.

2.4. Pulmonary artery anatomy and flow

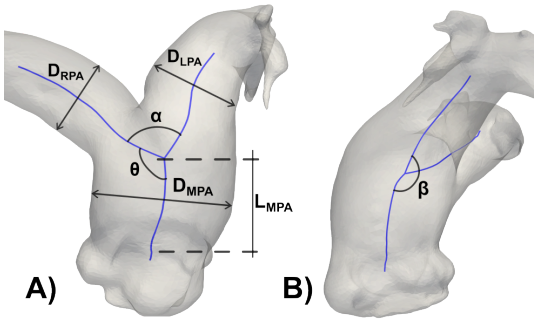

Figure 1. A) Front, and B) Side PA views, showing bifurcation angles, vessel diameters, and MPA length in Case 1.

3D surfaces of the proximal PA, consisting of a main trunk (MPA), and left and right branches (LPA, RPA), were manually segmented from CT images using Slicer[8, 9]. These meshes were used to characterize anatomy and flow, as described next. For anatomy, the Vascular Modeling Toolkit was used to extract centerlines and geometric parameters of the two patients' PA anatomies at initial and follow-up visits [10, 11]. To examine the vessel remodeling due to medication, angles α, β, and θ, MPA length, and MPA, LPA, and RPA maximum diameters were extracted. For flow, the metric of vortex duration time (t_{vortex}), previously shown to linearly relate to mPAP [12], and Wall shear stress (WSS), previously found to correlate with PA stiffness in PH [13], were inferred by Computational Flow Dynamic (CFD) simulations. For the setup of the latter, geometries, with added outlet extensions for computational stability, were meshed on ANSYS [14], using tetrahedral elements were used, along with a prismatic boundary layer, for near-wall resolution. An inlet velocity boundary condition was applied, extracted from 2D phase-contrast images of the MPA level. Three-element Windkessel models were applied at the LPA and RPA outlets, and tuned to outflow rates derived from 2D phase-contrast MR images at the respective branch levels. The Navier-Stokes equations were solved transiently in the fluid domain using ANSYS Fluent[14]. Blood was modelled as an incompressible Newtonian fluid with ρ = 1060 Kg/m3, and μ = 0.004 Pa.s. Finally, as a measure of arterial stiffness, pulse wave velocity (PWV) was calculated from the 2D phase contrast MR images, as the transit distance divided by transit time, between MPA and RPA flow curves peaks.

3. Results

3.1. RV function

PV loops for both subjects, before and after medication, are shown in Fig.2. In Case 1, RV function deteriorated;

SV was much larger (66 vs. 16 ml) but the RV was more dilated, with pressures almost constant. In Case 2, RV function improved with respect to pressure and volume, as expected in response to medication. Energetics parameters in Table 2 show that the RV exerted less power in Case 2.

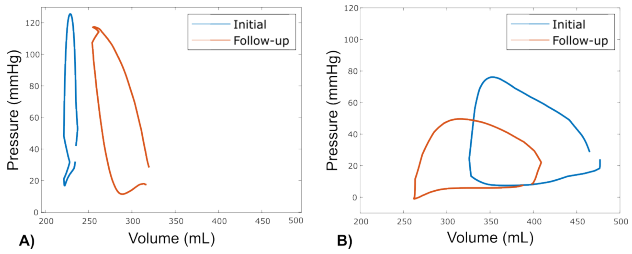

Figure 2. PV loops before medication (blue) and after two years of medication (orange) for a) Non-responder (Case 1), and b) Responder (Case 2).

Table 2. RV functional and energetics parameters. Volumes are in ml, powers in Watt.

Case/Visit	EDV/ESV	EF	SP	PO
1/Initial	237/221	0.07	0.780	0.270
1/F-U	320/254	0.21	0.638	0.253
2/Initial	477/326	0.32	0.431	0.288
2/F-U	410/262	0.36	0.183	0.177

3.2. RV-PA coupling

RV-PA coupling improved in both cases, but the increase in Case 2 was more pronounced (50% increase vs. 6% increase in Case 1), meaning that Case 2 was able to remodel towards a well-coupled system. The RVSPO ratio reveals that the energetic transfer between RV and pulmonary vasculature became more efficient in Case 2.

Table 3. Coupling efficiency. Elastances are in mmHg/ml.

Case/Visit	E_{es}	E_a	RV-PA	RVSPO ratio
1/Initial	2.06	6.14	0.34	0.35
1/F-U	0.83	4.22	0.36	0.40
2/Initial	0.14	0.35	0.40	0.67
2/F-U	0.11	0.19	0.60	0.97

3.3. PA shape and function

In Case 1, a large dilation of the MPA, RPA, and LPA (15%-45%) was observed with medication, while the bifurcation angles and MPA lengths changed only slightly (4%-7%). In Case 2, medication only caused a small dilation of the proximal PA arteries (1.7%-6%), but a larger change in bifurcation angles, namely in α, (13% change).

Table 4. Shape metrics. Angles in degrees, lengths in mm.

Case/Visit	$\alpha/\beta/\theta$	L_{MPA}	$D_{max,M/R/LPA}$
1/Initial	72/137/87	30	32.2/21.3/24.8
1/F-U	69/143/93	32	37.1/31.1/32.1
2/Initial	74/106/105	23	39.9/33.2/34.0
2/F-U	90/112/113	26	40.6/35.4/34.7

Stiffness estimators show that in Case 1 the average systolic WSS decreased in the MPA, indicating an increased stiffness. The opposite was seen in Case 2, where average systolic WSS increases and PWV decreases. In both cases the MPA right side WSS decreased with medication while the WSS on the MPA left side increased. The MPA vortex duration quantification from CFD revealed a slight increase in t_{vortex} in Case 1 (44% vs 43% of the cardiac cycle), and a decrease in duration in Case 2 (38% vs 41% of the cardiac cycle). These trends are consistent with the catheter-measured mPAP values.

Table 5. Flow parameters. PWV is in m/s, average systolic MPA WSS values are in $dynes/cm^2$.

Case/Visit	PWV	WSS_{right}/WSS_{left}	WSS_{mean}
1/Initial	7.8	3.55 / 2.85	3.20
1/F-U	8	2.39 / 2.92	2.66
2/Initial	5.7	3.10 / 5.23	4.17
2/F-U	4.2	2.43 / 6.40	4.40

4. Discussion

Results showed that Case 1 responded poorly to medication, while the response in Case 2 was as expected. In both cases, Treprostinil appeared to be doing its expected primary task, i.e. the reduction of afterload (PVR). However, in Case 1, this decrease was not reflected in the mPAP, which exhibited a 7% increase vs. a 16% decrease in Case 2. Additionally, in Case 1, this decrease in PVR did not strongly affect the RV. The RV function was severely impaired before drug administration, with very low values for SV and EF, therefore the slight relief caused by a decreased PVR, was still not sufficient to reverse the RV remodelling despite increasing the EF to 21%. Furthermore, the RV is more dilated at follow-up and the arterial elastance E_a was also high, meaning that the RV needed higher contractility to maintain coupling. However, RV-PA coupling in Case 1 was decreased at follow-up, and the energetic transfer,

represented by the RVSPO ratio was almost unchanged, further showing the inability of the system to cope with the disease stage. In Case 2, although the starting EDV and ESV were higher than in Case 1, RV function improved after drug administration, with both volumes and pressures decreasing. The system was significantly better coupled at follow-up, with more efficient RVSPO ratio, and decreased RV work. Flow patterns within the PA were then analyzed to understand why a decreased PVR was not accompanied by a similar decrease in mPAP in Case 1. Quantifying the MPA vortex duration revealed that the change in t_{vortex} was consistent with the small increase in pressure in Case 1, suggesting that t_{vortex} is not a direct translation of PVR, but rather a sign of other remodelling processes. This analysis suggests that vortex formation within the PA may be a more nuanced indicator of disease progression than PVR alone. It is also worth noting that in Case 1, where mPAP is quite high, the correlation observed *in-vivo* by [12] does not seem to hold. This suggests that in cases of severe PH the progressive decoupling of the system could affect the fluid topology in the MPA. The increase of PA stiffness observed in Case 1, quantified by PWV, may have also contributed to the pressure increase. MPA WSS was found to correlate with PA stiffness [13], in agreement with in our simulations. We note that our simulations assumes rigid walls, while the mentioned study was conducted on 4D Flow data. Lastly, PA remodelling was analyzed through shape metrics. The bifurcation angles in Case 2 exhibited more variability than in Case 1. Vessel dilation at follow-up was significantly higher in Case 1 than in Case 2, which could be an indicator of a compensatory mechanism to adapt to the disease since changes in downstream vasculature are insufficient. It appears that, overall, treatment was more effective in earlier stages of the disease. However, a larger cohort is needed to make strong claims.

Acknowledgments

Malak Sabry is supported by a PhD grant from Siemens Healthineers and the Magdi Yacoub Foundation.

References

[1] Nakaya T, Ohira H, Sato T, Watanabe T, Nishimura M, Oyama-Manabe N, Kato M, Ito YM, Tsujino I. Right ventriculo–pulmonary arterial uncoupling and poor outcomes in pulmonary arterial hypertension. Pulmonary Circulation 2020;10:2045894020957223.

[2] Zare P, Heller D. Treprostinil 2019;.

[3] Rischard F, Champion H, Vanderpool R, Waxman A, Hansen L, Jenkins I. Right ventriculo-arterial coupling in patients with pulmonary arterial hypertension undergoing rapid dose escalation of treprostinil. The Journal of Heart and Lung Transplantation 2014;33(4):S230.

[4] Vanderpool RR, Hunter KS, Insel M, Garcia JG, Bedrick EJ, Tedford RJ, Rischard FP. The right ventricular-pulmonary arterial coupling and diastolic function response to therapy in pulmonary arterial hypertension. Chest 2022; 161(4):1048–1059.

[5] Spazzapan M, Sastry P, Dunning J, Nordsletten D, De Vecchi A. The use of biophysical flow models in the surgical management of patients affected by chronic thromboembolic pulmonary hypertension. Frontiers in Physiology 2018;9:223.

[6] Sunagawa K, Maughan WL, Sagawa K. Optimal arterial resistance for the maximal stroke work studied in isolated canine left ventricle. Circulation Research 1985;56:586–95.

[7] Fernandes JF, Hammel JM, Zhou J, Xiao Y, Chen M, Alves R, Lof J, Grieve SM, Schuster A, Kuehne T, et al. Right ventricular energetics and power in pulmonary regurgitation vs. stenosis using four dimensional phase contrast magnetic resonance. International Journal of Cardiology 2018; 263:165–170.

[8] 3d slicer. URL `https://www.slicer.org/`.

[9] Fedorov A, Beichel R, Kalpathy-Cramer J, Finet J, Fillion-Robin JC, Pujol S, Bauer C, Jennings D, Fennessy F, Sonka M, et al. 3d slicer as an image computing platform for the quantitative imaging network. Magnetic Resonance Imaging 2012;30(9):1323–1341.

[10] Sabry M, Hermida U, Hassan A, Nagy M, Stojanovski D, Samuel I, Locas J, Yacoub MH, De Vecchi A, Lamata P. Exploring the relationship between pulmonary artery shape and pressure in pulmonary hypertension: A statistical shape analysis study. In Statistical Atlases and Computational Models of the Heart. Regular and CMRxRecon Challenge Papers. Springer Nature Switzerland, 2024; 186–195.

[11] Antiga L, Piccinelli M, Botti L, Ene-Iordache B, Remuzzi A, Steinman DA. An image-based modeling framework for patient-specific computational hemodynamics. Medical and Biological Eng and Computing 2008;46(11):1097–1112.

[12] Reiter G, Reiter U, Kovacs G, Kainz B, Schmidt K, Maier R, Olschewski H, Rienmueller R. Magnetic resonance derived 3-dimensional blood flow patterns in the main pulmonary artery as a marker of pulmonary hypertension and a measure of elevated mean pulmonary arterial pressure. Circulation Cardiovascular Imaging 2008;1(1):23–30.

[13] Schäfer M, Kheyfets VO, Schroeder JD, Dunning J, Shandas R, Buckner JK, Browning J, Hertzberg J, Hunter KS, Fenster BE. Main pulmonary arterial wall shear stress correlates with invasive hemodynamics and stiffness in pulmonary hypertension. Pulmonary Circulation 2016; 6(1):37–45.

[14] Ansys. URL `https://www.ansys.com/`.

Address for correspondence:

Malak Sabry, malaksabry@kcl.ac.uk
Saint Thomas' Hospital, London SE1 7EH, United Kingdom